Int J Legal Med (2012) 126:685–691
DOI 10.1007/s00414-012-0714-6

ORIGINAL ARTICLE

Geometric and harmonic study of the aging of the fourth rib

Laurent Fanton · Marie-Paule Gustin · Géraldine Maujean · Olivier Bernard · Norbert Telmon · Daniel Malicier

Received: 28 December 2011 / Accepted: 2 May 2012 / Published online: 17 May 2012

Abstract One of the current reference methods, namely the Işcan method for estimating age at death, consists in the subjective observation of the sternal end of the fourth rib. In this study, we looked to identify the morphometric characteristics of the sternal end of the fourth rib that were most affected by aging by measuring them in an objective way. For this purpose, we collected measurements from the fourth rib tip of 414 French males and used mathematical algorithms derived from pattern recognition and signal processing to identify variables that reflect both geometric characteristics and serration patterns of the ribs. Completed analysis was carried out on the 284 ribs for which all the variables could be collected. We showed that the three least collinear variables that best explain age objectively are the postero-superior pit depth, the fine serrations of the ovoid (delineating the pit shape), and its posterior flaring. This work provides a useful basis for subsequent studies on aging and age prediction.

Keywords Fourth rib · Aging · Geometric analysis · Fourier analysis

Introduction

One of the current reference methods to estimate the age at death of a mature adult, the observation of the sternal end of the fourth rib, was first proposed by Işcan in the 1980s from macroscopic [1, 2] observations. This method, based on a morphological examination, consists of assigning the rib to

Electronic supplementary material The online version of this article (doi:10.1007/s00414-012-0714-6) contains supplementary material, which is available to authorized users.

L. Fanton (✉) · G. Maujean · D. Malicier
Institut Universitaire de Médecine Légale, Université de Lyon, Université Claude-Bernard Lyon 1, 12 avenue Rockefeller, 69008 Lyon, France
e-mail: laurent.fanton@chu-lyon.fr

L. Fanton · O. Bernard
Université de Lyon, INSA Lyon, Laboratoire CREATIS, CNRS UMR 5220, INSERM U1044, INSA, avenue Jean Capelle, 69100 Villeurbanne, France

L. Fanton · N. Telmon
Université de Toulouse, Laboratoire AMIS, FRE 2960 CNRS, 37 allées Jules Guesde, 31073 Toulouse, France

M.-P. Gustin
Université de Lyon, Université Claude–Bernard Lyon 1, Institut des Sciences Pharmaceutiques, 8 avenue Rockefeller, 69008 Lyon, France

M.-P. Gustin
Service de Biostatistiques, Hospices Civils de Lyon, 162 avenue Lacassagne, 69003 Lyon, France

G. Maujean
Université de Lyon, Université Claude-Bernard Lyon 1, IGFL, UMR 5242, ENS Lyon, 46 allée d'Italie, 69007 Lyon, France

N. Telmon
Service de Médecine Légale, CHU Toulouse-Rangueil, 1 avenue Professeur Jean Poulhès, 31059 Toulouse Cedex 9, France

one of the nine phases described by Işcan, derived from age-related developmental changes noted at the costochondrial junction [3–5]. Yoder et al. then showed that this one could also be used on the right and left rib V–IX [6]. In practice, the sample is compared to three photographs that illustrate each phase and allow the evaluation of the pit depth, the pit shape and rim configurations, as well as the bone quality and thickness. Recently, we added to the criticisms leveled at this method of age estimation, highlighting its poor repeatability and reproducibility, which were nevertheless of less concern than the rather subjective aspect to observations of the variables, and also the underlying principles of the method [7]. The identification of one phase per decade from photographs appears poorly adapted to the ongoing nature of aging [8], nor does it allow for phenotypic variation in the sternal end of the rib to be taken into consideration. The judgment of these elements ultimately appears to depend not so much on explicit knowledge as on the implicit knowledge of the expert. Işcan's method was also found to be imprecise relative to the quality assurance criteria currently used for an age estimation method [9–12]. This imprecision is inherent to this type of method, since it is based on the observation of degenerative phenomena that present multifactorial variability among individuals [13]. The statistical methods of the time could not quantify this phenomenon nor define the precision of Işcan's method [8]. However, it was also observed that Işcan's variables did contain some objective information about age. The aim of this work was to select objective variables from the observation of the fourth rib that could best explain the age by using morphometric computational analysis to process variables with greater precision and objectivity.

Materials and method

A forensic sample of 414 right fourth ribs from males of French ethnicity (mean age, 49 years; wide range of age, 15–96 years) was collected for identification purposes from 2005 to 2008. The ribs were macerated in water until the soft tissue and cartilage were easily detached and then heated to 80 °C in a bain-marie of water until all remnant tissues were completely removed. The pits (in sagittal view) and the rims of each rib (in coronal view with 90° rotation) were photographed with a digital camera (Canon EOS Macro LENS F 100 mm 2.8 USM) at the same life-size scale. The calculations relative to the initial variables were made automatically using a computer program implemented in the MATLAB environment.

Pit shape delineated by an ovoid

From the photograph of the sagittal view of the pit (or cavity), an ovoid outline (denoted by ovoid) was traced using Photoshop 7.0® software (Adobe Systems Incorporated, San Jose, CA) (Fig. 1). Because of the irregularity of this ovoid, the principal vertical axis was drawn visually. The small transversal axis was defined by a segment traced at a perpendicular right angle to the principal vertical axis, from edge to edge of the ovoid and passing through the center point of the principle axis. This segment was broken down into an anterior axis and a posterior axis. From the principal axis, we calculated the anterior, posterior, and total surface areas. We then calculated three ratios detailed in Fig. 1: i.e., total, anterior, and posterior flaring of the ovoid. The higher these ratios are, the more the ovoid looks flattened. In the inverse case, it looks flared.

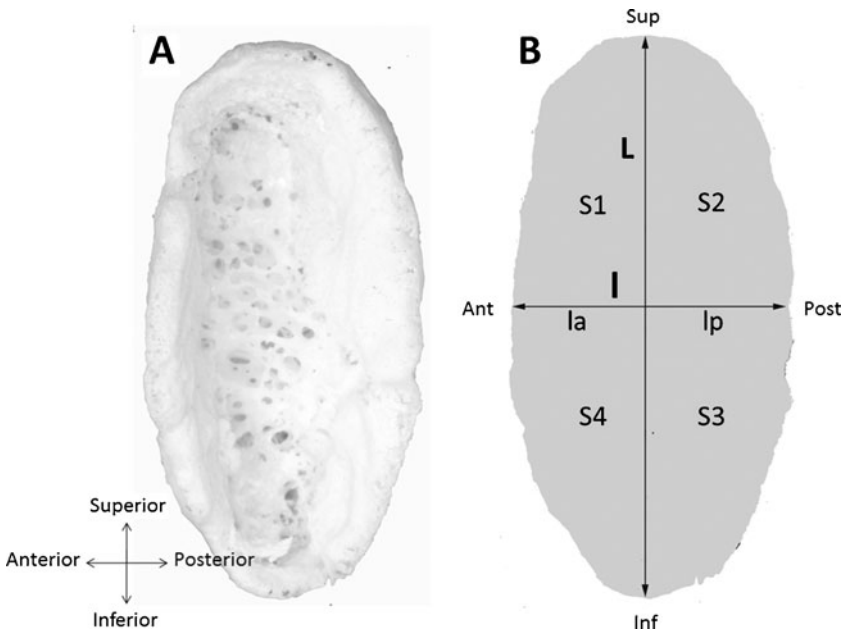

Fig. 1 Study of pit shape. Sagittal view of pit shape (**a**); ovoid (**b**) with principal vertical axis of length *L*, secondary horizontal axis of length *l*, secondary anterior axis of length *la*, and secondary posterior axis of length *lp*. These axes delimit four surface areas: S1, S2, S3, and S4. Total surface of the pit shape is defined as the sum of the anterior surface (S1+S4) and the posterior surface (S2+S3). Total, anterior, and posterior flaring of the ovoid are evaluated by the ratios L/l, L/la, and L/lp, respectively

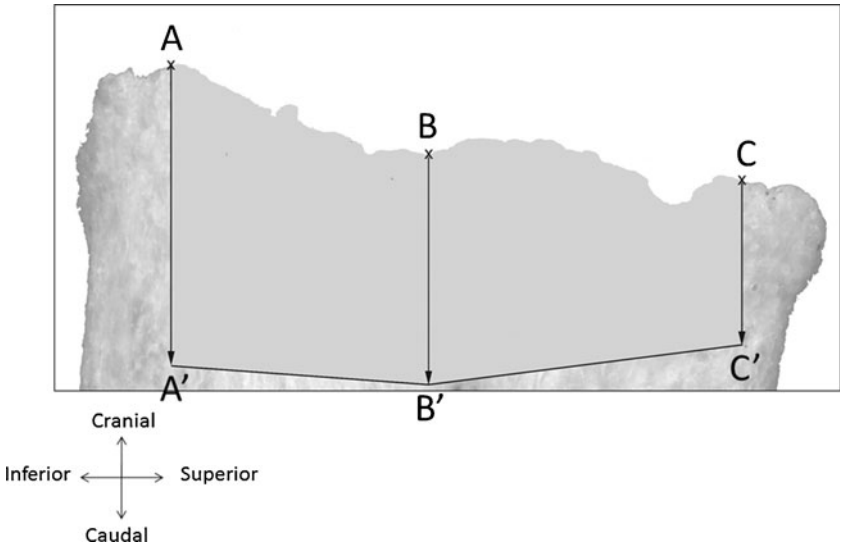

Fig. 2 Study of pit depth from a horizontal view of the posterior face. Points *A*, *B*, and *C* correspond to the three measurement points on the rim. The position of points *A′*, *B′*, *C′* were deduced from the measurements of pit depth at *A*, *B*, and *C*. For each face (anterior and posterior), mean superior and inferior pit depth were computed taking the surfaces of respectively [AA′B′B] and [BB′C′C] normalized by the number of pixels in accordance with the scale of the digitized photography

Pit depth

The depth of the pit was difficult to measure because of the irregularity of its rim and bottom, so average depths were calculated for the anterior and posterior sides. For each of these, three pit depths were measured manually with a caliper from points marked on the rim which were then transferred onto the corresponding digital photograph of the rib (Fig. 2). This enabled the identification of an inferior and a superior parallelepiped, and their surface areas, which were used to calculate average inferior and superior depths.

Outline of the pit rim

The outline of the rim presents irregular serrations (or indentations) depending on age. To quantify this phenomenon, we employed Fourier descriptors, a technique derived from spectral analysis and used to describe numerically shapes with closed contours, independent of scaling, translation, or rotation [14, 15]. This analysis, widely used for morphometric studies, decomposes the outline of the rim into a series of sine wave oscillations, allowing the size of the irregularities to be quantified according to their fineness (supplementary Fig. 1, pages 2–3). Calculations were performed for the rim in both sagittal and coronal views. For simplicity, we refer to the obtained variables as ovoid Fourier descriptors in sagittal view and as rim Fourier descriptors in coronal view (Fig. 3).

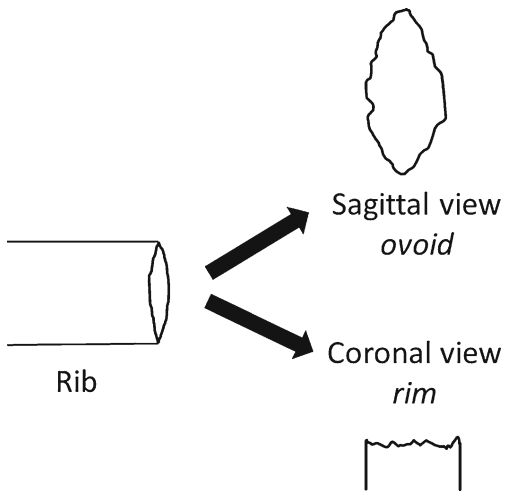

Fig. 3 Ovoid and rim terms are employed for the outline of the pit in sagittal and coronal views, respectively

Statistics

Statistical analysis is performed using the R language, version 2.12.2, available at http://cran.r-project.org.

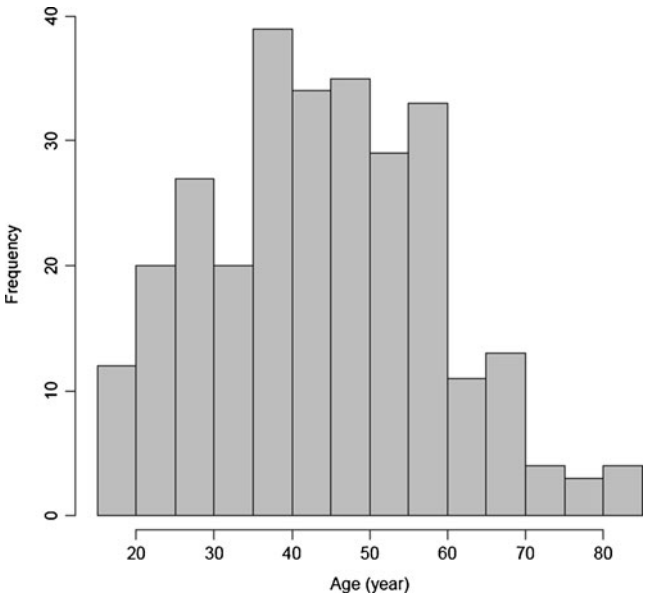

Fig. 4 Age histogram of the subsample, 284 males of French ethnicity

Table 1 Pearson correlation matrix of the six selected variables for the individuals with no missing values and no variable transformation (n=284)

Pearson Correlation	Age	Surf	Flaring	Depth	FDpit2	FDpitsup16	FDrim
Age	1	0.51	0.38	0.60	0.51	0.52	0.45
Surf		1	0.54	0.45	0.84	0.65	0.36
Flaring			1	0.34	0.57	0.25	0.28
Depth				1	0.45	0.38	0.47
FDpit2					1	0.63	0.35
FDpitsup16						1	0.48
FDrim							1

Surf postero-superior surface of the ovoid, *Flaring* posterior flaring of the ovoid, *Depth* postero-superior pit depth, *FDpit2* general curvature of the ovoid, *FDpitsup16* fine serrations of the ovoid, *FDrim* the fine serrations of the rim

First selection of variables

The first step was to determine which variables out of the primary ones correlated best with age. We listed the set of these variables in Supplementary data, page 3. We then obtained the adjusted Pearson correlation coefficient to compare the strength of the linear relationship between age and each variable in turn. We carried out special calculation for the Fourier descriptors detailed in Supplementary data, page 6. In certain cases, some individuals showing extreme values with high Cook's distance or high residuals were eliminated [16]. We then calculated the correlation matrix of the age and the most informative variables on age. At each step, only individuals without any missing values for the selected variables were entered in the computation. This subsample was of 284 ribs (mean age, 44 years; wide range of age, 15–83 years) (Fig. 4).

Second selection of variables

The partial correlation matrix was then estimated using the function cor2pcor of the R package corpcor. The partial correlation between two variables gives their correlation when maintaining the other variables constant; this allows evidencing of any "direct" link between two variables. The four variables that best correlate partially with age were kept. Then, we deeply analyzed their correlation with age to improve correlation by potential logarithm transformation. Variable normality was tested by the Shapiro–Wilk test.

Multiple regression

We then performed a stepwise multiple regression starting from the saturated model including the four best partially correlated variables with age, their square, and their interactions. Iterations were stopped when the residual sum of squares for two successive nested models was not significantly reduced at 5 %. The function lm of the R base package was used for estimating the different models.

Results

First variable selection

Six variables were selected at the first step of the analysis and were relevant to the posterior part of the joint. For clarity, we avoid using the term "posterior" in the variables. We retained the surface of the ovoid, its flaring, the postero-superior pit depth, the general curvature of the ovoid, its fine serrations, and the fine serrations of the rim. This first selection is detailed in the Supplementary data, pages 4–8. Table 1 shows that all pairwise correlations of these variables are significant at 5 %, evidencing their high collinearity. The pit depth and the variables that gave the general geometry of the ovoid (surface and flaring) were highly correlated to each other (r range, 0.34–0.60, n=284). The ovoid surface is highly correlated with its general curvature (r=0.84), reflecting its correspondence with the general shape of the pit. The fine serrations of the ovoid correlate with its surface (r=0.65)

Table 2 Pairwise partial correlation between age and each variable with no missing values and no variables transformation (n=284)

Partial correlation	Age	Surf	Flaring	*Depth*	FDpit2	*FDpitsup16*	*FDrim*
Age	1	0.03	0.12	0.40	0.04	0.22	0.10

Surf postero-superior surface of the ovoid, *Flaring* posterior flaring of the ovoid, *Depth* postero-superior pit depth, FDpit2 general curvature of the ovoid, *FDpitsup16* fine serrations of the ovoid, *FDrim* the fine serrations of the rim

The four selected variables for further multiple regression analysis are italicized

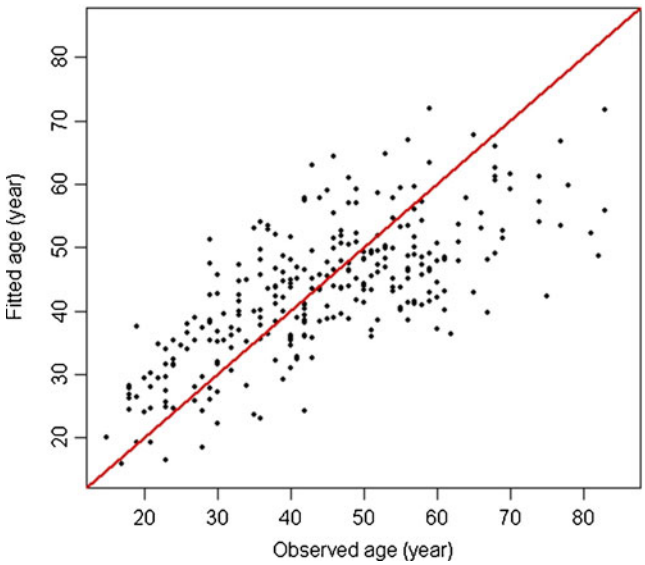

Fig. 5 Fitted versus observed plots for the age using the selected model by stepwise multiple regression (n=284). The *plain line* corresponds to the principal diagonal

whereas the fine serrations of the rim correlate with the pit depth (r=0.47). As we will discuss, these results are a consequence of the aging process.

Second variable selection

Table 2 gives the partial correlation of the six previously selected variables with age. The four best partial correlations with age are observed with depth (r=0.40, n=284), with the fine serrations of the ovoid (r=0.22), with the flaring of the ovoid (r=0.12), and the fine serrations of the rim (r=0.10). The response variable, age, and the explanatory variables, except the flaring, were logarithmically transformed before performing the multiple regression (Supplementary data, pages 9–10).

Multiple regression analysis

The model selected by stepwise multiple regression conserved the four simple effects (i.e., the four previously selected variables) and only one interaction between the pit depth and the ovoid fine serrations (Supplementary data, pages 11–12). The model is given by the following equation:

$$\log(\text{age}) = 0.36 + 1.35\log(x_1) + 0.74\log(x_2) + 0.11x_3 + 0.07\log(x_4) - 0.29\log(x_1)$$

with x_1 denoting the postero-superior pit depth, x_2 the fine serrations of the ovoid, x_3 the posterior flaring of the ovoid, x_4 the fine serrations of the rim, and $\log(x_1)/\log(x_2)$ the interaction between the logarithms of x_1 and x_2.

Note that the two best explanatory variables (depth and fine serrations of the ovoid, $p<10^{-2}$) showed a weak partial correlation (pr range, −0.01 to 0.14) so they can be considered as not directly linked (Supplementary Table 5). The model explained 55 % of the variability of age from these four variables: the pit depth, the ovoid flaring, the ovoid fine serrations, and the rim. This percentage fell by more than half in a model without the three most significant. So, the greater part of the explanation of age came from the three preceding variables, pit depth, ovoid flaring, and fine serrations of the rim, that gave complementary information. From a predictive point of view, the model showed a tendency to overestimate the age of young individuals and underestimate the age of the oldest ones as most of the models in anthropology [8] (Fig. 5).

Discussion

In this paper, we propose a selection of objective variables that give the best information on age at death from the sternal end of the fourth rib. We tried to collect the maximum amount of objective information by favoring the accuracy and the reliability of measurements.

We could only obtain the full set of variables for 70 % (284 of 414) of the ribs. The problems encountered were mainly due to bony projections that prevented us from appreciating (or estimating) correctly the outline of the ovoid or the rim depending on the case. Because of these projections that had expanded with age, the distribution of individuals' age has been slightly shifted (towards younger subjects). So, the ribs with measurement difficulties were mostly those of older subjects (Supplementary data, pages 13–14).

Pit depth was particularly difficult to obtain. We could not get easily three correct measurement points because of the bony projections on the rim. We calculated a mean pit depth to cope with the irregularities of the pit bottom that might lead to an over- or underestimation of the depth in case of a single measure point. Işcan himself suggested that pit depth should not be taken into account in future studies, whereas we found this variable to be the most informative one. This justifies our method of measurement. Furthermore, we are currently carrying out a study using image segmentation techniques which will allow us to obtain measurements for all the variables whatever the form of the rib articulation.

As for all bones of the body, the rib tends to enlarge with age [17–19]. This explains the increase of the whole surface of its cavity (or ovoid). In addition, the primary variables that correlated the best with age were all related to the

posterior part of the cavity. The eversion of the wall is indeed greater for the posterior part of the rib. The effect of this eversion is an increase of the posterior surface and of the supero-posterior pit depth. This asymmetry is likely due to the mechanical constraints on the joint during respiration movements that are more important on the supero-posterior part of the rib.

There are irregularities of the outline of the cavity or the rim that increase with age. This was evidenced by the fine ovoid and rim serrations. Our results confirmed Işcan's observations by highlighting the increase of fine serrations with age. These serrations are more visible on the posterior part of the rib in sagittal view, likely because of the phenomenon of eversion.

Taken together, these phenomena of cavity or rim deformations are caused by a reaction of the bone around mechanically constrained cartilage [20, 21] and site of a degeneration that makes the bone more rigid and fragile [22, 23]. By analogy with what might be observed in an enarthrosis joint, they can be compared to osteophytic spurs [24–26].

The three most significant variables of the multiple regression model that "explain" age (pit depth, ovoid fine serrations, and rim flaring) bring partly complementary information. Particularly, the presence of fine serrations is likely linked to other characteristics of the individuals that determine the depth or the ovoid flaring. The "explanatory" capacity of the model remained limited (R^2=55 %). As the pit depth was not always obtained but was sufficiently correlated with the posterior surface of the ovoid, we might replace the depth with the surface in the model. In this way, the "explanatory" capacity of the model only fell by 11 % (R^2=44 %, data not shown).

From a predictive point of view, as the primary variables were highly correlated to each other, it might be that we could make a better prediction with a small number of new variables which could be linear combinations of our existing variables. The principal component regression [27] and partial least squares regression [28] did not improve the residual standard error (data not shown). In addition, despite the more stable results with such shrinkage method, the new variables calculated in the regression are difficult to interpret.

Our study showed that we can evidence characteristics due to aging that are shared by most of the individuals. However, aging does not develop at the same speed according to individuals. This explains the difficulties of predicting age even from reliable objective variables. It appears necessary to reintroduce a pattern analysis by experts. This information could complement the information given by the objective measures that we have presented.

Acknowledgments We thank Professor Christian Paultre for his valuable contribution to the experimental setup as well as to the interpretation of results and Robert Grant for the translation and editing of the paper.

References

1. Kerley ER (1970) Estimation of skeletal age: after about age 30 years. In: Stewart TD (ed) Personnal identification in mass disaster. National Museum of Natural History, Washington, DC, pp 57–70
2. Ubelaker DH (1978) Human skeletal remains: excavation, analysis, interpretation. Aldine Pub Co, Chicago, p. 116
3. Işcan MY, Loth SR, Wright RK (1984) Metamorphosis at the sternal rib end: a new method to estimate age at death in white males. Am J Phys Anthropol 65:147–156
4. Işcan MY, Loth SR, Wright RK (1984) Age estimation from the rib by phase analysis: white males. J Forensic Sci 29:1094–1104
5. Işcan MY, Loth SR (1985) Age estimation from the rib by phase analysis: white females. J Forensic Sci 30:853–863
6. Yoder C, Ubelaker DH, Powell JF (2001) Examination of variation in sternal rib end morphology relevant to age assessment. J Forensic Sci 46(2):223–227
7. Fanton L, Gustin MP, Paultre U, Schrag B, Malicier D (2010) Critical study of the observation of the sternal end of the right 4th rib. J Forensic Sci 55(2):467–472
8. Schmitt A, Murail P, Cunha E, Rougé D (2002) Variability of the pattern of aging on the human skeleton: evidence from bone indicators and implications on age at death estimation. J Forensic Sci 47(6):1203–1209
9. Ritz-Timme S, Cattaneo C, Collins MJ, Waite ER, Schütz HW, Kaatsch HJ, Borrman HIM (2000) Age estimation: the state of the art in relation to the specific demands of forensic practise. Int J Legal Med 113:129–136
10. Rösing FW, Graw M, Marré B, Ritz-Timme S, Rotschild MA, Rötzscher K, Schmeling A, Schröder I, Geserick G (2007) Recommendations for the forensic diagnosis of sex and age from skeletons. Homo 58:75–78
11. Schmeling A, Geserick G, Reisinger W, Olze A (2007) Age estimation. Forensic Sci Int 165:178–182
12. Rissech C, Wilson J, Winburn AP, Turbón SD (2012) A comparaison of three established age estimation methods on an adult Spanish sample. Int J Legal Med 126:145–155
13. Schmitt A (2002) Estimation de l'âge au décès des sujets adultes à partir du squelette: des raisons d'espérer. Bull Mém Soc Anthropol Paris XIV(1–2):51–73
14. Duerk JL (1999) Principles of MR images formation and reconstruction. Magn Reson Imaging Clin N Am 7(4):629–659
15. Brown RA, Frayne R (2008) A comparaison of texture quantification techniques based on the Fourier and S transform. Med Phys 35 (11):4998–5008
16. Cook J, Stefanski L (1994) Simulation-extrapolation estimation in parametric measurement error models. J Am Stat Ass 89:1314–1328
17. Epker BN, Kelin M, Frost HM (1965) Magnitude and location of cortical bone loss in human rib with aging. Clin Orthop 41:198–203
18. Sedlin E, Viallanueva AR, Frost HM (1963) Age variations in the specific surface of Howship's lacunae as an index of human bone resorption. Anat Rec 146:201–207
19. Smith RW, Walker RR (1964) Femoral expansion in aging women: implications for osteoporosis and fractures. Science 145:156–157
20. Semine AA, Damon A (1975) Costochondral ossification and aging in five populations. Hum Biol 47(1):101–116
21. King JB (1939) Calcification of the costal cartilages. Brit J Radiol 12:2–12

22. Hough AJ, Mottram FC, Sokoloff L (1973) The collagenous nature of amianthoid degeneration of human costal cartilage. Am J Pathol 73:201–216
23. Sokoloff L (1966) Elasticity of aging cartilage. Fed Pro 25 (3):1089–1095
24. Menkes CJ, Lane NE (2004) Are osteophytes good or bad? Osteoarthr Cartil 12(Suppl A):S53–S54
25. Das SK, Farooqi A (2008) Osteoarthritis. Best Pract Res Clin Rheumatol 22(4):657–675
26. Kawaguchi H (2008) Endochondral ossification signals in cartilage degradation during osteoarthritis progression in experimental mouse models. Mol Cells 25(1):1–6
27. Johnson RA, Wichern DW (2007) Applied multivariate statistical analysis, 6th edn. Prentice Hall, New Jersey, 767 pp
28. Wold S, Ruhe A, Wold H, Dunn W (1984) The collinearity problem in linear regression: the partial least squares (pls) approach to generalized inverses. SIAM J Sci Stat Comp 5:735–743